EQUINE VETERINARY JOURNAL
Equine vet. J. (2008) **40** (1) 00-00
doi: 10.2746/042516408X322166

Computed tomographic anatomy of the temporomandibular joint in the young horse

M. J. RODRÍGUEZ*, R. LATORRE†, O. LÓPEZ-ALBORS†, M. SOLER, C. AGUIRRE, J. M. VÁZQUEZ†, M. QUEROL‡ and **A. AGUT**

Department of Medicine and Surgery, Veterinary School, University of Murcia, 30100 Espinardo, Murcia, Spain; †Department of Anatomy, Veterinary School, University of Murcia, 30100 Espinardo, Murcia, Spain; ‡and Resonancia de Murcia, Medicina y Gestión Sanitaria, S.L., Murcia, Spain.

Keywords: horse; temporomandibular joint; computed tomography; anatomy; cross-sectional imaging

Summary

Reasons for performing study: **The equine temporomandibular joint (TMJ) and its surrounding structures can be difficult to investigate in cases with a clinical problem related to the region. Little previous attention has been given either to a computed tomographic (CT) imaging protocol for the joint or an interpretation of the structures displayed in CT images of the normal joint.**

Objectives: **To provide a CT atlas of the normal cross-sectional anatomy of the equine TMJ using frozen and plastinated sections as anatomical reference.**

Methods: **Eight TMJs from 4 immature pure-bred Spanish horses were examined by helical CT. Scans were processed with a detailed algorithm to enhance bony and soft tissue. Transverse CT images were reformatted into sagittal and dorsal planes. Transverse, sagittal and dorsal cryosections were then obtained, photographed and plastinated. Relevant anatomic structures were identified in the CT images and corresponding anatomical sections.**

Results: **In the CT images, a bone window provided excellent bone detail, however, the soft tissue components of the TMJ were not as well visualised using a soft tissue window. The articular cartilage was observed as a hyperattenuating stripe over the low attenuated subchondral bone and good delineation was obtained between cortex and medulla. The tympanic and petrous part of the temporal bone (middle and inner ear) and the temporohyoid joint were seen in close proximity to the TMJ.**

Conclusions: **Helical CT provided excellent images of the TMJ bone components to characterise the CT anatomy of the normal joint.**

Potential relevance: **Detailed information is provided that may be used as a reference by equine veterinarians for the CT investigation of the equine TMJ and serve to assist them in the diagnosis of disorders of the TMJ and related structures (middle and inner ear). The study was performed at an immature stage and further studies of mature individuals are required in order to confirm that the clinical interpretation is not affected by changes occurring with age.**

Introduction

The equine temporomandibular joint (TMJ) and its surrounding structures form a complex anatomical region that can be difficult to investigate in cases presented with a clinical problem related to the site (Ramzan 2006; Rodríguez *et al*. 2007). Previous reports have described the anatomy (May *et al*. 2001; Weller *et al*. 2002; Rodríguez *et al*. 2006) and biomechanical functions (Bonin *et al*. 2006, 2007) of the joint. The equine TMJ is a synovial condylar articulation between the temporal bone and the mandible; its main articular components are the 2 noncommunicating synovial pouches (dorsal and ventral synovial pouches), the articular disc, lateral and caudal ligaments, and joint capsule (Nickel *et al*. 1986; Weller *et al*. 2002). Other key related structures are the TMJ masticatory muscles (*temporalis*, masseter, lateral and medial pterygoid: Rodríguez *et al*. 2006), vascular (superficial temporal artery and vein, pterygoid venus plexus, and transverse facial vessels: Barone 1980) and neural structures (facial nerve, mandibular and masseteric: Barone 1980) and the middle ear (Rodríguez *et al*. 2006).

Reports of TMJ diseases are sparse in horses, possibly due to these disorders being undiagnosed since this relies on heteroanamnesis, and clinical signs that can be confused with neurological or behavioural problems, including headshaking, quidding, masticatory problems or dysphagia (Warmerdam *et al*. 1997; Devine *et al*. 2005; Nagy and Simhofer 2006). The principal published disorders of the equine TMJ have been fractures (Devine *et al*. 2005), luxations (Hurtig *et al*. 1984; Hardy and Shiroma 1991), and septic and nonseptic arthritis (Carmalt and Wilson 2005; Nagy and Simhofer 2006). Radiography (Townsend and Cotton 2007), scintigraphy (Weller *et al*. 1999a), computed tomography (Rosenstein *et al*. 2001; Devine *et al*. 2005; Nagy and Simhofer 2006) and ultrasonography (Weller *et al*. 1999a; Rodríguez *et al*. 2007) are valuable imaging methods with which to evaluate the equine TMJ thoroughly.

Conventional radiography has been the standard procedure to image the TMJ in the horse, but the superimposition of the adjacent osseous structures, difficulties in positioning for multiple views and the complex anatomy of the equine head often impairs interpretation of radiographic views (Weller *et al*. 1999b). Novel imaging methods (computerised tomography [CT] and magnetic

*Author to whom correspondence should be addressed.
[Paper received for publication 30.10.07; Accepted 21.02.08]

resonance imaging [MRI]) have been developed to avoid overlapping and distortion of the anatomical features of the joint, which could provide more reliable assessment of this region (Devine *et al*. 2005; Nagy and Simhofer 2006). CT is very useful for assessing the bony components of the TMJ and, in human studies, offers high sensitivity and specificity (Tsiklakis *et al*. 2004). Furthermore, thanks to the recent development of multislice helical CT (MSCT), it has been possible to obtain 3D reformatted images allowing a realistic and spatially accurate reconstruction of TMJ structures. Such 3D images provide supplementary useful structural and functional information and lead to more effective therapy (Kau *et al*. 2005; Casanova *et al*. 2006).

However, a thorough knowledge of anatomy of the TMJ region is a prerequisite for obtaining accurate interpretation of CT images. Previous reports have shown the usefulness of CT for demonstrating equine TMJ disorders (Warmerdam *et al*. 1997; Devine *et al*. 2005; Nagy and Simhofer 2006), but they have not provided a detailed description of the anatomy of the TMJ as demonstrated in the CT images. The purpose of the current study was to provide an atlas of the CT anatomy of the normal equine TMJ; frozen and plastinated sections were used to confirm the CT findings.

Materials and methods

Animals

CT images were obtained of 8 TMJs from 4 immature pure-bred Spanish horses (age 1–3 years; 238–427 kg bodyweight), subjected to euthanasia for reasons not related to a TMJ disorder. Horses with dental disorders, masticatory muscle diseases and other related mouth pathology were excluded because of the potential damage over the TMJ (ref?). Each head was separated from the body at the atlanto-occipital level to enable their evaluation in an upright position; and the TMJs were examined ultrasonographically to rule out the presence of joint effusion or bony irregularity that could indicate a TMJ abnormality. Ultrasonography was performed with an ultrasonographic unit[1] and an 11 MHz linear-array transducer. The protocol described by Weller *et al*. (1999a) and Rodríguez *et al*. (2007) was followed in this study.

Computed tomographic study

The CT evaluation of the heads was performed within 2 h of euthanasia to avoid *post mortem* changes. The heads were placed in an upright position with the image plane perpendicular to the dorsal plane of the head. A helical CT scanner (CT HiSpeed CT/e Dual)[2] was employed (120 kV and 130 mA; pitch = 1; collimation = 2 mm; gantry rotation = 1.5 s). Contiguous 1 mm transverse slices were acquired starting at the most rostral aspect of the zygomatic process of the temporal bone and continuing caudally up to the occipital condyles of the skull. Scans were processed with a detailed algorithm to enhance bony and soft tissues using an appropriate window (a wide window for bone and a narrow window for soft tissue).

Transverse CT images were reformatted into sagittal and dorsal planes (MPVR software)[2]. The defined field of view was 25 cm with a pixel matrix of 512 x 512. The original data were stored and transferred to an image analysis workstation (ADW 4.1)[1] capable of generating 3D volume-rendered reconstructed images of the joint, using a standard DICOM 3D format[2]. The window width and level were adjusted as required to achieve optimal images.

Anatomical study

Following the scanning procedure, arteries, veins and synovial structures of the clipped and cleaned heads were injected with red, blue and green latex, respectively, using a peristaltic pump (Rodríguez *et al*. 2006). Each head was frozen at -30ºC for 48 h and then sectioned with a high-speed band saw in blocks containing only the TMJ. These blocks were frozen at -70ºC for one week to obtain contiguous 3 mm-thick transverse, sagittal and dorsal cryosections that were photographed and plastinated (Latorre *et al*. 2003).

The CT images and corresponding anatomic sections were correlated, and an internationally accepted nomenclature used for labelling all structures (Anon 1994).

Results

Ultrasonography showed that each TMJ was free of pathology, and that they had similar CT appearance with each anatomical component of the joint being identified and well correlated. Additionally, with volume-rendering reconstruction techniques, the 3D-CT images were rotated and sectioned as desired, contributing to better spatial visualisation of each TMJ (Figs 1A, 2A and 3A).

Blood vessels, such as the buccal vein, maxillary artery, transverse facial vessels, pterygoid venous plexus and caudal deep temporal vein were seen containing air (black colour), similar to the guttural pouches in bone and soft tissue CT images (Figs 1B, 2B and 3B).

Despite the employment of a soft tissue algorithm and windowing, the TMJ soft tissue components were not as well visualised as the bone-containing structures. It was possible, however, to identify and correlate the articular disc, caudal compartment of the dorsal synovial pouch, synovial fluid, articular capsule, and the relationship between the TMJ and masticatory muscles. Each of these soft tissues showed variable shades of grey and the synovial fluid was the lowest attenuating structure. It was not possible to identify the TMJ ligaments in CT images (Fig 3B), unlike in anatomical sections (Fig 3C).

The use of the bone window and detailed algorithm produced excellent images with high bone detail, so that clear differentiations could be made between the cortex (continuous flat high attenuating line) and medulla (homogeneous low attenuating structure); the trabecular pattern of the medullary bone was also well depicted. The articular cartilage was identified as a regular, smooth, high attenuating line over the homogeneous low attenuating subchondral bone (Figs 1B, 2B and 3B).

On transverse CT (Fig 1B) and anatomical sections (Fig 1C), the articular surfaces (articular cartilage and subchondral bone), articular space and lateromedial axis of the joint were assessed. Relationships were identified between the TMJ and the adjacent medial structures (i.e. the petrous and tympanic parts of the temporal bone [inner and middle ear], temporohyoid joint, guttural pouches, maxillary artery and its pterygoid branches, internal carotid artery, temporal venous sinus, pterygoid venous plexus and caudal deep temporal vein). The parotid salivary gland, maxillary vein, transverse facial vessels and facial nerve were in close proximity to the lateral aspect of the TMJ. However, the transverse anatomical sections revealed more valuable information that was not identifiable in the CT images including the topography of the mandibular and masticatory nerves.

Dorsal CT images (Fig 2B) allowed evaluation of the lateromedial axis of the mandibular condyle and articular space. The articular cartilage, subchondral bone, external auditory meatus, middle and inner ear, and temporohyoid joint were also easily evaluated (Fig 2C).

The rostrocaudal location of condyle in relation to mandibular fossa was examined on sagittal images (Fig 3B and 3C). The cross-sectional area of articular cartilage and subchondral bone displayed on sagittal CT images was smaller than the cross-sectional area of these components shown on transverse and dorsal CT images. The relationship between the TMJ and the temporohyoid joint, middle and inner ear was visualised. Likewise, in the anatomical sections, the caudal fibrous expansion of the articular disc and the caudal ligament of the articular capsule were well observed and also their relationship with the guttural pouch wall and superficial temporal vein and artery. The caudal ligament of the articular capsule was not visualised in CT images. The rostral compartments of the dorsal and ventral synovial pouches were clearly identified in the CT images (Fig 3B).

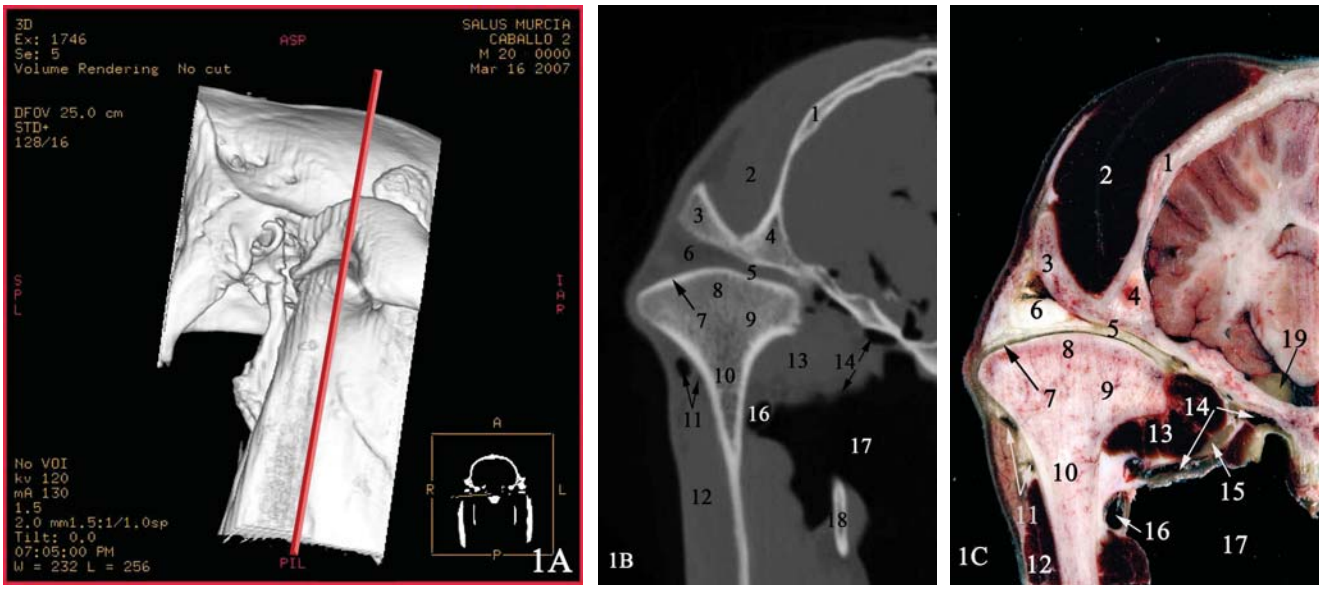

Fig 1: (A) Volume rendered 3D-reformatted image of the lateral aspect of the right TMJ showing a transverse-sectional plane of reference for Figures 1B and 1C; (B) Bone window transverse CT image (window width = 2354; window level= 154) and (C) transverse anatomical section (caudal aspect) of the right TMJ. The progression of CT and anatomical images was from rostral to caudal, from the level of the most rostral aspect of the zygomatic arch. The orientation of CT and anatomic sections is consistent: the right side is to the viewer's left and dorsal is at the top of the image. 1 = parietal bone; 2 = temporal muscle; 3 = zygomatic process of the temporal bone; 4 = squamous part of the temporal bone; 5 = articular disc; 6 = caudal compartment of the dorsal synovial pouch (intra-articular fat tissue); 7 = articular cartilage; 8 = subchondral bone; 9 = mandibular condyle; 10 = ramus of the mandible (spongy bone); 11 = transverse facial vessels; 12 = masseter muscle; 13 = lateral pterygoid muscle; 14 = pterygoid venous plexus and maxillary artery, 15 = mandibular nerve; 16 = buccal vein; 17 = guttural pouch; 18 = stylohyoid bone; 19 = trigeminal nerve.

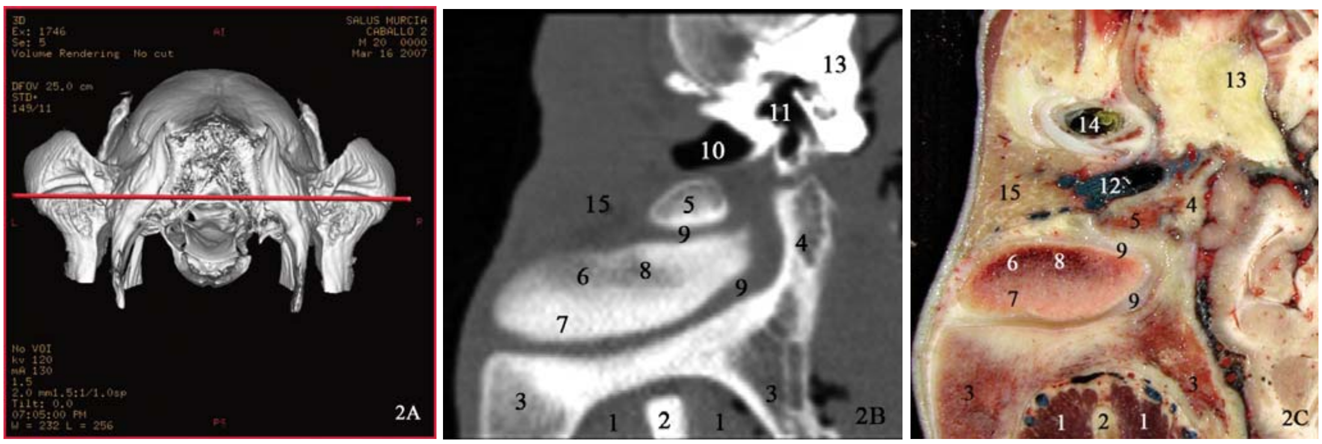

Fig 2: (A) Volume rendered 3D-reformatted image of the dorsal view of the right TMJ showing a dorsal-sectional plane of reference for Figures 2B and 2C; (B) Bone window dorsal CT image (window width = 2354; window level= 154) and (C) dorsal anatomical section (dorsal aspect) of the right TMJ. The progression of CT and anatomical images was from dorsal to ventral aspect. The lateral aspect is on the left side and the caudal aspect at the top of the image. 1 = temporal muscle; 2 = coronoid process; 3 = zygomatic process of the temporal bone; 4 = squamous part of the temporal bone; 5 = retroarticular process; 6 = mandibular condyle; 7 = articular cartilage; 8 = subchondral bone; 9 = articular disc; 10 = guttural pouch; 11 = tympanic part of the temporal bone (middle ear); 12 = caudal deep temporal vein; 13 = petrous part of the temporal bone; 14 = external auditory meatus; 15 = parotid salivary gland.

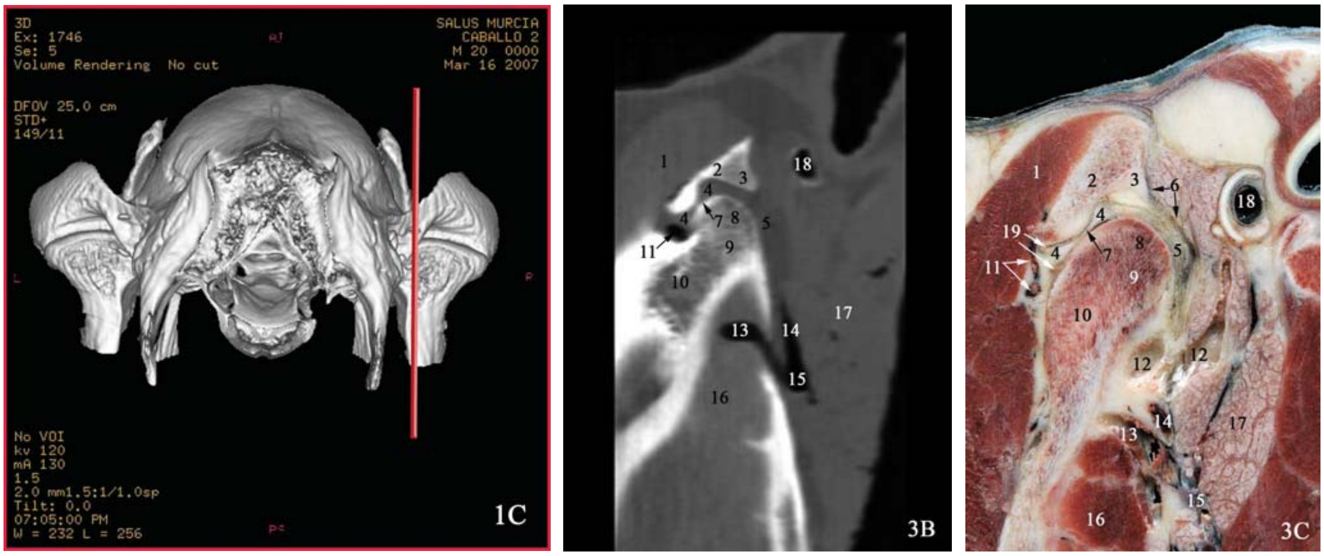

Fig 3: (A) Volume rendered 3D-reformatted image of the caudal view of the right TMJ showing a sagittal-sectional plane of reference for Figures 3B and 3C; (B) Bone window sagittal CT image (window width = 2354; window level= 154) and (C) sagittal anatomical section (lateral aspect) of the right TMJ. The progression of the CT and anatomical images was from lateral to medial aspect. The lateral aspect is on the top and dorsal aspect to the left side of the image. 1 = temporal muscle; 2 = zygomatic process of the temporal bone; 3 = retroarticular process; 4 = articular disc; 5 = caudal fibrous expansion of the articular disc; 6 = articular capsule (caudal ligament); 7 = articular cartilage; 8 = subchondral bone; 9 = mandibular condyle; 10 = ramus of the mandible; 11 = caudal deep temporal vessels; 12 = guttural pouch (wall); 13 = buccal vein; 14 = superficial temporal vein; 15 = maxillary vein; 16 = masseter muscle; 17 = parotid salivary gland; 18 = external auditory meatus; 19 = rostral compartment of the dorsal and ventral synovial pouches.

Discussion

The TMJ is an essential part of the masticatory system (Bonin *et al*. 2007) and knowledge of its morphology and function is fundamental to understanding of its role in equine mouth disorders (Ramzan 2006). The diagnosis of TMJ diseases can be an arduous process and where diagnostic images have been obtained, their interpretation can be far from straightforward (Ramzan 2006). CT is a valuable imaging modality that is increasingly used in equine medicine to diagnose bone and joint diseases (Ruohoniemi *et al*. 1997; Tomlinson *et al*. 2003). In dogs and cats, CT is also burgeoning but there are few reports regarding CT imaging of the TMJ (Schwarz *et al*. 2002; Beam *et al*. 2007).

The protocol used for this study was based on the reports of TMJ computed tomography in human medicine (Honey *et al*. 2007; Vilanova *et al*. 2007). The high resolution dual-helical CT unit used enabled successful evaluation of the TMJ components. The quality of the obtained images for bone was excellent using a bone windowing and detailed algorithm. A narrow soft tissue window and detailed algorithm clearly delineated the masticatory muscles, as reported by other authors (Arencibia *et al*. 2000; Morrow *et al*. 2000; Devine *et al*. 2005). The articular disc, articular capsule and the caudal compartment of the dorsal synovial pouch were difficult to visualise and the ligaments of the TMJ were not seen in the CT images in the present study. These results differed from descriptions of TMJ soft tissues in man (Kaga *et al*. 2003; Kau *et al*. 2005; Casanova *et al*. 2006), probably because more advanced CT scanners (3D cone beam CT) were used, which provided a more highly focused X-ray beam, higher contrast resolution and a reduction in scattered radiation than helical CT units (Seeram 2001; Honda *et al*. 2001; Honey *et al*. 2007). These more advanced CT units also lead to a reduction in scan time and radiation exposure (Westerman 2001). In the present study, several criteria were used to reduce the presence of image artefacts and increase image contrast resolution, including thin anatomical slices (1 mm), higher x-ray parameters and detailed imaged algorithms (Nugent and Keobke 2001). However, the resultant images did not reach satisfactory contrast resolution to permit a well-defined visualisation of the TMJ soft tissues.

The horses used for the study were immature and variations of the TMJ CT appearance were not demonstrated. Warmerdam *et al*. (1997) described 2 septic arthritis in 2 horses, one mature and the other immature, diagnosed by CT. In spite of being pathological situations, the authors did not report differences between the scans. However, further studies concerning the CT appearance of the equine TMJ are needed to assess the influence of age, in order to confirm the clinical relevance of changes observed in relation to pathology.

In horses, the principal disadvantages of CT imaging are related to the availability of the equipment and the need for general anaesthesia (Puchalski 2006). Fortunately, portable CT units have been developed for use in the standing horse, which may lead to more widespread use of the imaging method (McIlwraith 2003). A thorough knowledge of the anatomy is required for the proper interpretation of CT images of the equine TMJ (Arencibia *et al*. 2000; Morrow *et al*. 2000; Smallwood *et al*. 2002). In the current study, frozen and plastinated anatomical sections were used to assist in the interpretation and establish accurate correlations with the CT images; such plastinated sections have also been useful in the interpretation of other different imaging methods in other medical fields (Latorre and Rodríguez 2007).

The CT images poorly delineated the soft tissue structure, associated with the TMJ, and such a finding may be related to the difference between the density of TMJ soft tissues and that of the surrounding bony tissue (Seeram 2001). Recent studies of other anatomical regions in the horse, such as the carpus, tarsus and distal extremity, described the potential of CT to evaluate soft tissue structures including the vasculature (Kaser-Hotz *et al*. 1994; Tomlinson *et al*. 2003; Collins *et al*. 2004). These authors claimed that CT provided a good soft tissue texture assessment which was sufficient for a specific diagnosis. Currently, to obtain better delineation of soft tissues, an iodinated contrast medium has also been used (Collins *et al*. 2004; Puchalski *et al*. 2007).

In the present study, to minimise soft tissue findings associated with *post mortem* change, the CT study was performed within 2 h of euthanasia; however, several venous vessels were air-filled in the images. The air accumulation was attributed to *post mortem* changes as described by Morrow *et al*. (2000). These findings should be recognised since, in clinical cases, normal vessels appear hypoattenuated owing to their fluid-content (Kaser-Hotz *et al*. 1994). Other findings on the TMJs CT images that could be attributed to *post mortem* changes, which modified the imaging reference, were not identified in our study. Reports of CT imaging of the head in mature horses and foals (Morrow *et al*. 2000; Smallwood *et al*. 2002) did not mention any characteristic *post portem* variation of the TMJ's appearance.

Transverse, sagittal and dorsal CT images were obtained in the anatomical study of the TMJ. Transverse and sagittal CT views provided more information about the articular surface and position of the condyle, mandibular fossa and retro-articular process, similar to human results (Yu *et al*. 2004; Casanova *et al*. 2006), where these planes were recommended to evaluate the TMJ space and the surface of the mandibular condyle. Dorsal images were useful to assess the articular cartilage, subchondral bone and symmetry of the articular space. In man, the dorsal view is used to confirm or refute suspicion of a lesion seen on the transverse view (Nugent and Keobke 2001). The volume-3D reconstructed images were helpful to visualise all 3 planes of the joint and the surface characteristics (Kau *et al*. 2005; Tucker and Sande 2002).

In conclusion, helical computed tomography is an excellent method for the detailed assessment of the bony structures of the equine TMJ. The current study did not, however, produce high resolution images of the TMJ soft tissues. The information provided by this study might be useful as a primary protocol for the CT study of the equine TMJ and could be used to assist clinicians in the interpretation the images.

Manufacturers' addresses

[1]General Electric Co., Waukesha, Wisconsin, USA.
[2]Toshiba Medical Systems, Zoetermeer, The Netherlands.

References

Anon (1994) *Nomina Anatomica Veterinaria,* 4th edn., International Committee on Veterinary Gross Anatomical Nomenclature, World Association of Veterinary Anatomists, Ithaca. pp 1-198.

Arencibia, A., Vázquez, J.M., Rivero, M., Latorre, R., Sandoval, J.A., Vilar, J.M., and Ramírez, J.A. (2000) Computed tomography of normal cranioencephalic structures in two horses. *Anat. Histol. Embryol.* **29**, 295-299.

Barone, R. (Ed) (1980) Articulations de la tête. Muscles masticatours. In: *Anatomie Comparée des Mammifères Domestiques*, Vol. 2: *Arthrologie et Miologie*, 2nd edn., *Editions Vigot,* Paris. pp 28-34, 467-476.

Beam, R.C., Kunz, D.A., Cook, C.R., Carson, R.L., Briscoe, P. and Cook, J.L. (2007) Use of three-dimensional computed tomography for diagnosis and treatment planning for open-mouth jaw locking in a cat. *J. Am. vet. med. Ass.* **230**, 59-63.

Bonin, S.J., Clayton, H.M., Lanovaz, J.L. and Johnson, T.J. (2006) Kinematics of the equine temporomandibular joint. *Am. J. vet. Res.* **67**, 423-428.

Bonin, S.J., Clayton, H.M., Lanovaz, J.L. and Johnson, T.J. (2007) Comparison of mandibular motion in horses chewing hay and pellets. *Equine vet. J.* **39**, 258-262.

Carmalt, J.L. and Wilson, D.G. (2005) Arthroscopic treatment of temporomandibular joint sepsis in a horse. *Vet. Surg.* **34**, 55-58.

Casanova, M.S., Tuji, F.M., Ortega, A.I., Yoo, H.J. and Haiter-Neto, F. (2006) Computed tomography of the TMJ in diagnosis of ankylosis: two case reports. *Med. oral Pathol. oral Cir. Bucal* **11**, E-413-416.

Collins, J.N., Galuppo, L.D., Thomas H.L., Wisner, E.R. and Hornof, W.J. (2004) Use of computed tomography angiography to evaluate the vascular anatomy of the distal portion of the forelimb of horses. *Am. J. vet. Res.* **65**, 1409-1420.

Devine, D.V., Moll, H.D. and Bahr, R.J. (2005) Fracture, luxation, and chronic septic arthritis of the temporomandibular joint in a juvenile horse. *J. vet. Dent.* **22**, 96-99.

Hardy, J. and Shiroma, J. (1991) What is your diagnosis? Rostral luxation of the right temporomandibular joint. *J. Am. vet. med. Ass.* **198**, 1663-1664.

Honda, K., Larheim, T.A., Johannessen, S., Arai, Y., Shinoda, K. and Westesson, P. (2001) Ortho cubic super-high resolution computed tomography: a new radiographic technique with application to the temporomandibular joint. *Oral Surg. oral Med. oral Pathol. oral Radiol. Endod.* **91**, 239-243.

Honey, O.B., Scarfe, W.C., Hilgers, M.J., Klueber, K., Silveira, A.M., Haskell, B.S. and Farman, A.G. (2007) Accuracy of cone-beam computed tomography imaging of the temporomandibular joint: comparisons with panoramic radiology and linear tomography. *Am. J. Orthod. dentofacial Orthop.* **132**, 429-438.

Hurtig, M., Barber, S. and Farrow, C. (1984) Temporomandibular joint luxation in a horse. *J. Am. vet. med. Ass.* **185**, 78-80.

Kaga, K., Takegoshi, H., Yamasoba, T., Nakamura, M., Kaneko, M. and Ino, K. (2003) Aplasia of zygomatic arch and dislocation of temporomandibular joint capsule in Treacher-Collins syndrome: three-dimensional reconstruction of computed tomographic scans. *Int. J. pediatr. Otorhinolaryngol.* **67**, 1189-1194.

Kau, C.H., Richmond, S., Palomo, J.M. and Hans, M.G. (2005) Three-dimensional cone beam computerized tomography in orthodontics. *J. Orthod.* **32**, 282-293.

Kaser-Hotz, B., Sartoretti-Schefer, S. and Weiss, R. (1994) Computed tomography and magnetic resonance imaging of the normal equine carpus. *Vet. Radiol. Ultrasound* **35**, 457-461.

Latorre, R., Arencibia, A., Gil, F., Rivero, M., Ramírez, G., Vázquez-Autón, J.M. and Henry, R.W. (2003) P-40 and S-10 plastinated slices: an aid to interpreting MR images. *J. Int. Soc. Plastination* **18**, 14-22.

Latorre, R. and Rodríguez, M.J. (2007) In search of clinical truths: equine and comparative studies of anatomy. *Equine vet. J.* **39**, 263-268.

May, K.A., Moll, H.D., Howard, R.D., Pleasant, R.S. and Gregg, J.M. (2001) Arthroscopic anatomy of the equine temporomandibular joint. *Vet. Surg.* **30**, 564-571.

McIlwraith, C.W. (2003) Advanced techniques in the diagnosis of bone disease. Kentucky equine research nutrition conference.In: *Advances in Equine Nutrition III,* Ed: J.D. Pagan, Nottingham University Press, Nottingham. pp 1-11.

Morrow, K.L., Park, R.D., Spurgeon, T.L., Stashak, T.S. and Arceneaux, B. (2000) Computed tomographic imaging of the equine head. *Vet. Radiol. Ultrasound* **41**, 491-497.

Nagy, A.D. and Simhofer, H. (2006) Mandibular condylectomy and meniscectomy for the treatment of septic temporomandibular joint arthritis in a horse. *Vet. Surg.* **35**, 663-668.

Nickel, R., Schummer, A. and Seiferle, E. (1986) Articulations of the bones of the head. Muscles of the mastication and superficial mandibular muscles. In: *The Anatomy of the Domestic Animals: The Locomotor System, Vol. 1,* 5th edn., Editions Verlag Paul Parey, Berlin and Hamburg. pp 172-173, 257.

Nugent, R.A. and Keobke, D. (2001) Computed tomography of the head, neck and spine. In: *Computed tomography: Physical Principles, Clinical Applications and Quality Control,* 2nd edn., Ed: E. Seeram, W.B. Saunders, Philadelphia. pp 331-332.

Puchalski, S. (2006) Computed tomographic and ultrasonographic examination of equine dental structures: normal and abnormal findings. In: *AAEP Focus Meeting*.

Puchalski, S.M., Galuppo, L.D., Hornof, W.J. and Wisner, E.R. (2007) Intraarterial contrast-enhanced computed tomography of the equine distal extremity. *Vet. Radiol. Ultrasound* **48**, 21-29.

Ramzan, P.H.L. (2006) The temporomandibular joint: component of clinical complexity. *Equine vet. J.* **38**, 102-104.

Rodríguez, M.J., Agut, A., Gil, F. and Latorre, R. (2006) Anatomy of the equine temporomandibular joint: study by gross dissection, vascular injection and section. *Equine vet. J.* **38**, 143-147.

Rodríguez, M.J., Soler, M., Latorre, R., Gil, F. and Agut, A. (2007) Ultrasonographic anatomy of the temporomandibular joint in healthy Pure Bred Spanish horses. *Vet. Radiol. Ultrasound* **48**, 149-154.

Rosenstein, S., Bullock, F., Ocello, J. and Clayton, M. (2001) Arthrocentesis of the temporomandibular joint in adult horses. *Am. J. vet. Res.* **62**, 729-735.

Ruohoniemi, M., Kärkkäinen, M. and Tervahartiala, P. (1997) Evaluation of the variable ossified collateral cartilages of the distal phalanx and adjacent anatomic structures in the Finnhorse with computed tomography and magnetic resonante imaging. *Vet. Radiol. Ultrasound* **38**, 344-351.

Schwarz, T., Weller, R., Dickie, A., Konar, M. and Sullivan, M. (2002) Imaging of the canine and feline temporomandibular joint: a review. *Vet. Radiol. Ultrasound* **43**, 85-97.

Seeram, E. (2001) Physical principles of computed tomography. In: *Computed tomography: Physical Principles, Clinical Applications and Quality Control,* 2nd edn., Ed: E. Seeram, W.B. Saunders, Philadelphia. pp 73-74, 176-186, 196-197.

Smallwood, J.E., Wood, B.C., Taylor, W.E. and Tate, L.P. (2002) Anatomic reference for computed tomography of the head of the foal. *Vet. Radiol. Ultrasound* **43**, 99-117.

Tomlinson, J.E., Redding, W.R., Berry, C. and Smallwood, J.E. (2003) Computed tomographic anatomy of the equine tarsus. *Vet. Radiol. Ultrasound* **44**, 174-178.

Townsend, N.B. and Cotton, J.C. (2007) A novel radiographic technique for investigation of the equine temporomandibular joint. In: *Proceeding of the 46th British Equine Veterinary Congress,* Equine Veterinary Journal Ltd, Newmarket. p 424.

Tsiklakis, K., Syriopoulos, K. and Stamatakis, H.C. (2004) Radiographic examination of the temporomandibular joint using cone beam computed tomography. *Dentomaxillofac. Radiol.* **33**, 196-201.

Tucker, R. and Sande, R. (2002) MRI, CT provide early link to diagnosing injuries, disease in horses. *dvm In Focus*, November 2002, 43-48.

Vilanova, J.C., Barceló, J., Puig, J., Remollo, S., Nicolau, C. and Bru, C. (2007) Diagnostic imaging: Magnetic resonance imaging, computed tomography, and ultrasound. *Semin. Ultrasound CT MR*, **28**, 184-191.

Warmerdam, E., Klein, W. and van Herpen, B. (1997) Infectious temporomandibular joint disease in the horse: computed tomographic diagnosis and treatment of two cases. *Vet. Rec.* **141**, 172-174.

Weller, R., Taylor, S., Maierl, J., Cauvin, E. and May, S. (1999a) Ultrasonographic anatomy of the equine temporomandibular joint. *Equine vet. J.* **31**, 529-532-

Weller, R., Cauvin, E.R., Bowen, I.M. and May, S.A. (1999b) Comparison of radiography, scintigraphy and Ultrasonography in the diagnosis of a case of temporomandibular joint arthropathy in a horse. *Vet. Rec.* **144**, 377-379.

Weller, R., Maierl, J., Bowen, I.M., May, S.A. and Liebich, H.G. (2002) The arthroscopic approach and intra-articular anatomy of the equine temporomandibular joint. *Equine vet. J.* **34**, 421-424.

Westerman, B.R. (2001) Advances in volume scanning. Multislice spiral/helical computed tomography: physical principles and instrumentation. In: *Computed tomography: Physical Principles, Clinical Applications and Quality Control,*2nd edn., Ed: E. Seeram, W.B. Saunders, Philadelphia. pp 242-249, 262-265.

Yu, Q., Yang, J., Wang, P., Shi, H. and Luo, J. (2004) CT features of synovial chondromatosis in the temporomandibular joint. *Oral Surg. oral Med. oral Pathol.* **97**, 524-528.

Author contributions: